Nicotinic Receptors on Local Circuit Neurons in Dentate Gyrus: A Potential Role in Regulation of Granule Cell Excitability

Charles J. Frazier, Ben W. Strowbridge and Roger L. Papke

You might find this additional info useful...

This article cites 31 articles, 16 of which you can access for free at:
http://jn.physiology.org/content/89/6/3018.full#ref-list-1

This article has been cited by 14 other HighWire-hosted articles:
http://jn.physiology.org/content/89/6/3018#cited-by

Updated information and services including high resolution figures, can be found at:
http://jn.physiology.org/content/89/6/3018.full

Additional material and information about *Journal of Neurophysiology* can be found at:
http://www.the-aps.org/publications/jn

This information is current as of August 8, 2016.

Nicotinic Receptors on Local Circuit Neurons in Dentate Gyrus: A Potential Role in Regulation of Granule Cell Excitability

Charles J. Frazier,[1] Ben W. Strowbridge,[2] and Roger L. Papke[1,3]

[1]*Department of Pharmacology and Therapeutics and* [3]*Department of Neuroscience, University of Florida, Gainesville, Florida 32610-0267; and* [2]*Department of Neurosciences, Case Western Reserve University, Cleveland, Ohio 44106*

Frazier, Charles J., Ben W. Strowbridge, and Roger L. Papke.
Nicotinic receptors on local circuit neurons in dentate gyrus: a potential role in regulation of granule cell excitability. *J Neurophysiol* 89: 3018–3028, 2003. First published February 12, 2003; 10.1152/jn.01036.2002. Although the dentate gyrus is one of the primary targets of septo-hippocampal cholinergic afferents, relatively little is known about the cholinergic physiology of neurons in the area. By combining whole cell patch-clamp recording with brief local application of exogenous agonists in horizontal slices, we found that there is robust expression of functional somatic α7-containing nicotinic acetylcholine receptors (nAChRs) on molecular layer interneurons, hilar interneurons, and the glutamatergic mossy cells of the dentate hilus. In contrast, the principal neurons of the dentate gyrus, the granule cells, are generally unresponsive to focal somatic or dendritic application of ACh in the presence of atropine. We also demonstrate that cholinergic activation of α7-containing nAChRs on the subgranular interneurons of the hilus can produce methyllycaconitine-sensitive GABAergic inhibitory postsynaptic currents (IPSCs) in nearby granule cells and enhance the amplitude of an electrically evoked monosynaptic IPSC. Further, activation of α7-containing nAChRs on subgranular interneurons that is timed to coincide with synaptic release of glutamate onto these cells will enhance the functional inhibition of granule cells. These findings suggest that a complex interplay between glutamatergic afferents from the entorhinal cortex and cholinergic afferents from the medial septum could be involved in the normal regulation of granule cell function. Such a relationship between these two afferent pathways could be highly relevant to the study of both age-related memory dysfunction and disorders involving regulation of excitability, such as temporal lobe epilepsy.

INTRODUCTION

Nicotinic acetylcholine receptors (nAChRs) are expressed in abundance throughout the CNS and have been associated with positive effects on attention, cognition, and working memory. Changes in function or expression of nAChRs have been implicated in Alzheimer's disease, schizophrenia, and some forms of epilepsy (Bertrand 1999; Elmslie et al. 1997). Although the functional neurophysiology of nAChRs has proven to be a challenging research topic, great progress has been made in recent years, particularly with respect to nAChRs that contain the α7 subunit. Several lines of evidence suggest a potential role for this receptor in volume transmission (Descarries et al. 1997; Uteshev et al. 2002), however; specific functional roles for α7 containing nAChRs have also been identified at both presynaptic and postsynaptic sites in hippocampus and elsewhere (Alkondon et al. 1998; Aramakis and Metherate 1998; Frazier et al. 1998a; Gray et al. 1996; Hatton and Yang 2002; Radcliffe et al. 1999). In CA1, these receptors are robustly expressed by local circuit neurons (Frazier et al. 1998b; Jones and Yakel 1997; McQuiston and Madison 1999), where they can be activated by endogenous release of ACh (Alkondon et al. 1998; Frazier et al. 1998a) and have been implicated in both inhibition and disinhibition of pyramidal cells (Buhler and Dunwiddie 2002; Ji and Dani 2000). Similarly, functional expression of nAChRs has been reported on hilar interneurons but not on principal neurons in the dentate gyrus (Jones and Yakel 1997). Recently, apparently very sparse expression of nAChRs has been detected on the apical dendrites of CA1 pyramidal cells and implicated in the induction of long-term potentiation (Ji et al. 2001). Indeed, recent immunological studies on the ultrastructural distribution and expression of α7 nAChRs in hippocampus and elsewhere have suggested that their role in mediating and modulating synaptic transmission may yet be underappreciated (Fabian-Fine et al. 2001; Levy and Aoki 2002).

This is likely to be particularly true in the dentate gyrus, an area that receives extensive cholinergic innervation and that has been a center of attention for research targeted at both age-related memory dysfunction and temporal lobe epilepsy. The principal neurons of the dentate gyrus, the granule cells, are activated by glutamatergic afferents that arrive from the entorhinal cortex via the perforant path (Johnston and Amaral 1998) and are connected by strong recurrent excitatory connections that likely occur via an unusual type of excitatory local circuit neuron in the dentate hilus, the mossy cells (Buckmaster et al. 1992, 1996; Jackson and Scharfman 1996). These cells, along with the GABAergic hilar interneurons, play a key role in regulation of granule cell excitability and are implicated in numerous theories regarding epileptogenesis. Recent dual-labeling immunoelectron microscopy studies have indicated that septohippocampal cholinergic afferents form conventional synapses on both mossy cells and hilar interneurons (Deller et al. 1999; Dougherty and Milner 1999). Based on a combination of the evidence reviewed here, we decided to examine each major cell type in the dentate gyrus for functional expression of nAChRs and to test the hypothesis that activation of such

receptors could be important in the regulation of granule cell excitability.

METHODS

Horizontal slices (300 μm) were prepared from 18- to 28-day-old Sprague Dawley rats using a vibratome (Pelco, Redding, CA). Slices were incubated at 30°C for 30 min and then maintained submerged at room temperature. The artificial cerebral spinal fluid (ACSF) used for cutting and incubating slices contained (in mM) 124 NaCl, 2.5 KCl, 1.2 NaH$_2$PO$_4$, 2.5 MgSO$_4$, 10 D-glucose, 1 CaCl$_2$, and 25.9 NaHCO$_3$, saturated with 95% O$_2$-5% CO$_2$. After incubation, slices were transferred to a recording chamber where they were visualized with infrared differential interference contrast microscopy (IR DIC) using a Nikon E600FN microscope and superfused at a rate of 2 ml/min with ACSF that was heated to 30°C and contained (in mM) 126 NaCl, 3 KCl, 1.2 NaH$_2$PO$_4$, 1.5 MgSO$_4$, 11 D-glucose, 2.4 CaCl$_2$, and 25.9 NaHCO$_3$, saturated with 95% O$_2$-5% CO$_2$. In experiments presented in Figs. 5–7, this solution was modified slightly to contain (in mM) 124 NaCl, 5 KCl, 1.2 NaH$_2$PO$_4$, 1.2 MgSO$_4$, 10 D-glucose, 2.5 CaCl$_2$, and 25.9 NaHCO$_3$. Whole cell patch-clamp recordings were made with pipettes pulled on a Flaming/Brown electrode puller (Sutter Instruments, Novato, CA). Pipettes were typically 3–5 MΩ when filled with an internal solution that contained (in mM) 140 Cs-MeSO$_3$, 8 NaCl, 1 MgCl$_2$, 0.2 EGTA, 10 HEPES, 2 MgATP, 0.3 Na$_3$GTP, and 5 QX-314. This solution prevented action potentials from occurring and allowed for stable voltage-clamp recording at depolarized membrane potentials. Access resistance was typically between 10 and 40 MΩ. Access resistance, input resistance, whole cell capacitance, and membrane time constant were all calculated from whole cell capacitive transients generated in voltage clamp by 20 mV depolarizations lasting 10–100 ms from a holding potential of –80 mV. For current-clamp recordings, a K-gluconate solution was used that contained (in mM) 125 K-gluconate, 1 KCl, 0.1 CaCl$_2$, 2 MgCl$_2$, 1 EGTA, 2 MgATP, 0.3 Na$_3$GTP, and 10 HEPES. All internal solutions were pH adjusted to 7.3 using additional CsOH or KOH, and volume was adjusted to ~285 mOsm. For experiments involving fluorescence microscopy, sulforhodamine 101 was added to the internal solution, and neurons were visualized using light from a mercury lamp filtered at 510–560 nm. For all local application experiments, a picospritzer (Gerneral Valve, Fairfield, NJ) was used to apply acetylcholine (1 mM), glutamate (1 mM), or choline (10 mM) from pipettes identical to those used for whole cell recording or from double-barreled pipettes made using theta tubing (Sutter Instruments, Novato, CA). When using single-barrel pipettes, agonists were applied for 5–15 ms using a pressure of 20–25 psi. When using double-barreled pipettes, time or pressure was occasionally increased beyond these values to obtain visual confirmation of robust application. Evoked responses were generated at 15-s intervals using a concentric bipolar stimulator (Frederick Haer, Bowdoinham, ME), connected to a constant current stimulus isolator (World Precision Instruments, Sarasota, FL). Current intensity varied between 50 and 300 μA, as necessary to generate reliable evoked responses. Stimuli lasted 0.1 ms. An Axon Multiclamp 700A amplifier (Axon Instruments, Union City, CA) was used to amplify voltage and current records. The data were sampled at 20 kHz, filtered at 2 kHz, and recorded on a computer via a Digidata 1200A A/D converter using Clampex version 8 or 9 (Axon Instruments). Data were analyzed using Clampfit version 8 or 9 (Axon Instruments), OriginPro v. 7.0 (OriginLab, Boston, MA), Graphpad Prism v. 3.0 (Graphpad Software, San Diego, CA), and Excel 2000 (Microsoft, Seattle, WA). All chemicals used in these experiments were obtained from Sigma (St. Louis, MO) except for 2,3-dioxo-6-nitro-1,2,3,4-tetrahydrobenzo[f]quinoxaline-7-sulfonamide disodium (NBQX), which was obtained from Tocris (Ellisville, MO).

RESULTS

Identification of local circuit neurons in the dentate gyrus

Local circuit neurons in the dentate gyrus were divided into three broad categories (mossy cells, hilar interneurons, and molecular layer interneurons) on the basis of their location, morphology, and physiology. Because both hilar interneurons and the glutamatergic mossy cells are located in the hilar region, a combination of IR DIC, fluorescence microscopy, and whole cell recording in both voltage clamp and current clamp was used to make an accurate identification. Under IR DIC, mossy cells were often multipolar and were almost uniformly larger than hilar interneurons (average whole cell capacitance was 203 $\pm$ 12.2 pF for mossy cells vs. 89.3 $\pm$ 11.5 (SE) pF for hilar interneurons). On average, mossy cells also had lower input resistance and a slower membrane time constant than hilar interneurons (121 $\pm$ 10.5 MΩ, 5.1 $\pm$ 1.0 ms vs. 168 $\pm$ 9.2 MΩ, 2.7 $\pm$ 0.5 ms, respectively). Further, every cell identified as a mossy cell showed evidence of complex spines on the proximal dendrites when visualized with florescence microscopy (Fig. 1A), whereas hilar interneurons were usually, but not always, aspiny (Fig. 1B). In both cell types, spontaneous activity recorded under voltage clamp at –70 mV was blocked by glutamate receptor antagonists (Fig. 1, C and D); however, every cell categorized as a mossy cell exhibited a unique population of large amplitude spontaneous events that was lacking in interneurons. A representative amplitude distribution for each cell type is shown in Fig. 1, E and F. When current-clamp recordings were made using a K-gluconate based internal solution, it became apparent that neurons identified as mossy cells always demonstrated a robust hyperpolarization activated sag and usually showed relatively long interspike intervals and modest frequency accommodation during a maintained depolarization (Fig. 1E). In contrast, most cells classified as hilar interneurons failed to show a clear hyperpolarization activated sag and demonstrated shorter interspike intervals in response to moderate depolarization (Fig. 1F). All of these characteristics are generally consistent with previously published reports (Lubke et al. 1998; Scharfman 1992; Scharfman and Schwartzkroin 1988). On average, molecular layer interneurons were smaller than hilar interneurons or mossy cells (average whole cell capacitance was 41 $\pm$ 7.4 pF). Although they also lacked the large amplitude spontaneous events and proximal dendritic spines that were characteristic of mossy cells, their identification was greatly simplified by the presence of their soma in stratum moleculare. Most stratum moleculare interneurons in our dataset were located in the inner, or middle portion of the layer, i.e., in the half closest to the granule cell layer.

Local circuit neurons in the rat dentate gyrus express somatic α7 containing nAChRs

All three types of local circuit neurons produced robust responses to local application of ACh in the presence of atropine. Inward currents measured under voltage clamp at –70 mV had average peak amplitudes of 201 $\pm$ 24.2 pA for mossy cells ($n = 11$), 185 $\pm$ 41.7 pA for hilar interneurons ($n = 17$), and 119 $\pm$ 47.6 pA for molecular layer interneurons ($n = 5$, Fig. 2A). These currents showed strong inward rectification with 1–2 mM internal Mg^{2+} and a reversal potential near 0 mV

(Fig. 3, *A* and *B*). Average ACh-evoked current amplitudes in the presence of 20–50 nM methyllycaconitine (MLA) (an α7-selective nAChR antagonist) were $\leq$ 5 pA in each cell type and as such could not be distinguished from background noise (Fig. 2, *A* and *C*). In most cases, a concentration of 50 nM MLA was used due to the rapid and unambiguous nature of its block (see time course of a typical experiment in Fig. 3*C*). Although this concentration is largely selective for α7 nAChRs, it was possible to get a slower and yet equally thorough block, and somewhat more rapid recovery, by using lower concentrations of MLA (Fig. 3*B*). While this evidence clearly indicates that the ACh-induced currents that we observed in each type of local circuit neuron were mediated by α7-containing nAChRs, we did two additional experiments to further confirm this conclusion. In the first experiment, responses were elicited in both mossy cells and hilar interneurons

with local application of choline (10 mM), a α7-selective agonist (Papke et al. 1996). In each case, choline produced inward currents that were comparable to those produced by ACh and that were also completely blocked by the α7-selective antagonist MLA (Fig. 2, *B* and *C*). In the second experiment, bath-applied choline was used at concentrations of 20–40 μM to desensitize α7-containing nAChRs and thus reduce or eliminate responses to local application of ACh (data not shown). Both of these control experiments further strengthen our conclusion that the vast majority of nAChRs activated in our experiments are likely to contain the α7 subunit.

In 10 of 11 mossy cells, 9 of 17 hilar interneurons, and 4 of 5 molecular layer interneurons that produced α7 like currents in the presence of atropine, additional drugs were applied to eliminate the possibility that activation of presynaptic nAChRs was facilitating release of a transmitter that in turn produced the postsynaptic response. In most cases, either 10 μM NBQX or 6,7-dinitroquinoxaline-2,3-dione (DNQX) coupled with 40 μM D-2–amino–5-phosphonovaleric acid (APV) was used for this purpose. In some cases, 1 μM TTX or a combination of NBQX, APV, and TTX was used instead. The effectiveness of these drugs was quite obvious in experiments involving mossy cells, where it was necessary to block spontaneous excitatory events to resolve the responses to local application of ACh (see Fig. 1*C*). Figure 3*C* shows a typical experiment on a hilar interneuron in which NBQX and APV failed to reduce an ACh-evoked response that was subsequently blocked by MLA.

Note that the α7-expressing local circuit neurons reported here represent a strong majority of all neurons tested. In total, 11 of 11 mossy cells, 17 of 21 hilar interneurons, and 5 of 7 molecular layer interneurons produced currents mediated by somatic α7-containing nAChRs in response to local application
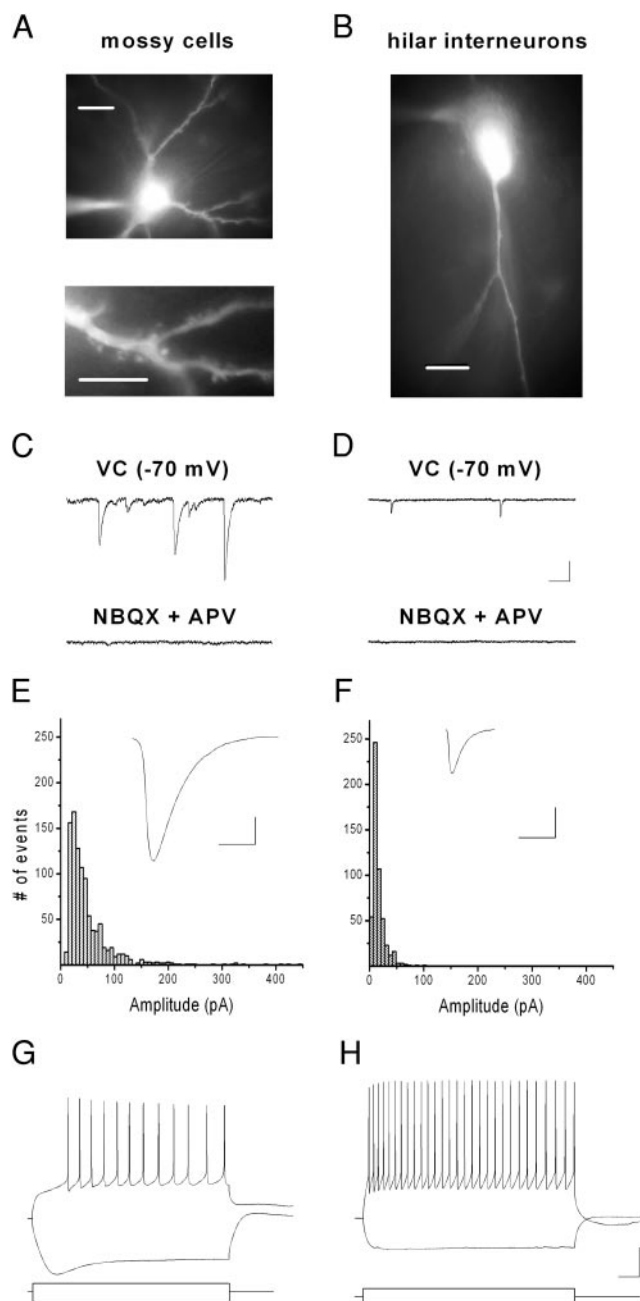

FIG. 1. Identification of local circuit neurons in the dentate hilus. *A, top*: a mossy cell filled with sulforhodamine 101 and visualized using fluorescence microscopy. Note the multipolar nature of this neuron. *Bottom*: a magnification of 1 of the dendritic branches that clearly indicates the presence of the dendritic spines that are characteristic of these neurons. *B*: a typical hilar interneuron visualized using identical techniques has fewer primary dendritic branches and is aspiny. *C*: a voltage-clamp recording at –70 mV from a mossy cell reveals large spontaneous events (*top*) that were blocked by glutamate receptor antagonists [10 μM 2,3-dioxo-6-nitro-1,2,3,4-tetrahydrobenzo[f]quinoxaline-7-sulfonamide disodium (NBQX) + 40 μM D-2–amino–5-phosphonovaleric acid (APV), *bottom*]. This type of activity was apparent in all mossy cells. *D*: lower amplitude spontaneous events recorded from hilar interneurons under identical conditions were also blocked by glutamate receptor antagonists. *E*: the amplitude distribution for all events recorded from the same mossy cell as in *C*. In total, 988 events were recorded over a 2-min time period. The amplitude of the events ranged from 11 to 445 pA, with an average event amplitude of 44.8 pA (*inset*). Nearly a third (30.9%) of the events exceeded 50 pA. *F*: in contrast, the amplitude distribution for all events recorded from the hilar interneuron in *D* over a 2-min time period indicates that a total of 521 events were recorded that ranged in amplitude from 6 to 100 pA, with an average event amplitude of 14.6 pA (*inset*). Only 1.9% of the events exceeded 50 pA. These data exemplify what was a consistent observation, i.e., that there was a unique population of large amplitude spontaneous glutamatergic events that was observed only in mossy cells. *E*: current-clamp recording from a mossy cell using a K-gluconate-based internal solution reveals the presence of a robust hyperpolarization activated sag (*bottom,* −200 pA for 1 s), whereas depolarization produced action potentials at a modest frequency (*top,* 160 pA for 1 s). *F*: most hilar interneurons lacked this hyperpolarization activated sag (*bottom,* −100 pA for 1 s) and fired action potentials more frequently in response to moderate depolarization (*top,* 150 pA for 1 s). Scale in *A*: 20 μm (*top*), 10 μm (*bottom*). Scale in *B*: 20 μm. Scale in *D*: 50 pA, 50 ms also applies to *C*. Scale insets for *E* and *F*: 10 pA, 100 ms. Scale in *H*: 20 mV or 500 pA, 100 ms also applies to *G*.
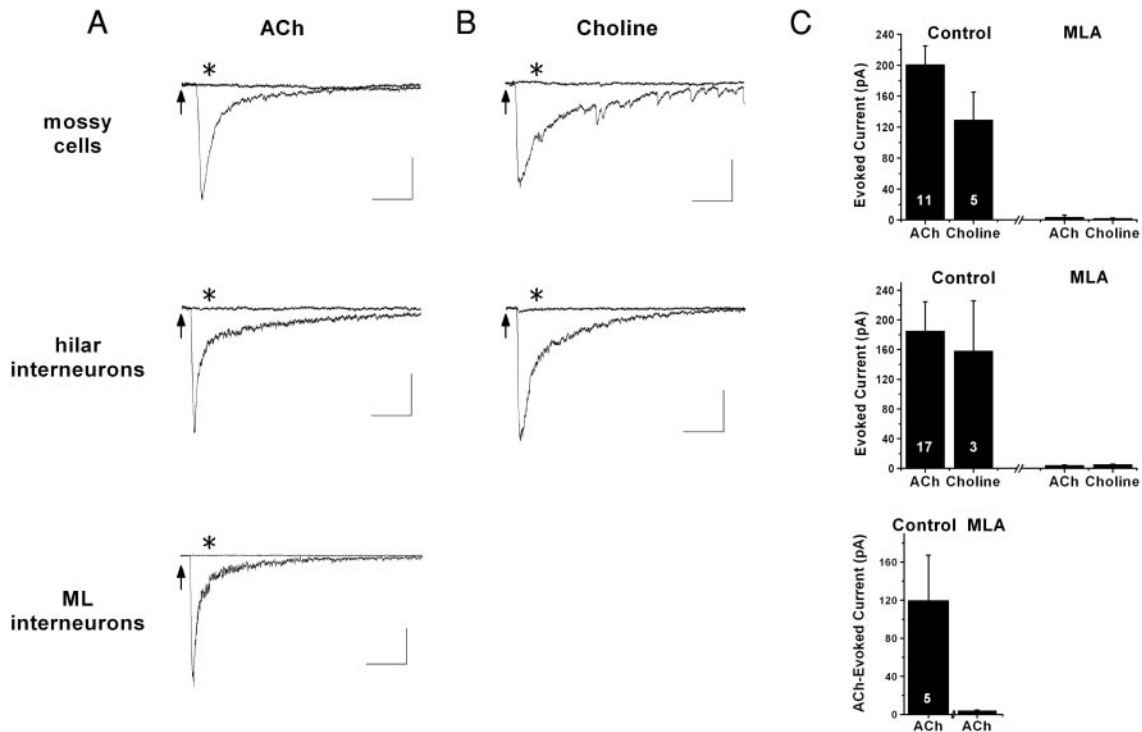
FIG. 2. Local circuit neurons in the dentate gyrus express somatic α7-containing nicotinic acetylcholine receptors (nAChRs). *A*: brief focal applications of 1 mM ACh (↑, 7.5–15 ms × ~20 psi) were delivered to the soma of local circuit neurons via a puffer pipette located within 5 μm of the cell body. In each panel, *bottom* represents the response to ACh, *top* (*) indicates the response to the same application of ACh after bath application of 50 nM methyllycaconitine (MLA). The labels on the left indicate the cell type. *B*: similar responses were produced by local application of 10 mM choline (*bottom*), an α7-selective nAChR agonist. Choline-evoked responses were also blocked by MLA (20–50 nM, *top*, *). 10 μM NBQX, 40 μM APV, 1 μM TTX, and 5 μM atropine were present in all experiments except for those on hilar interneurons in *A,* where only TTX and atropine were used. Each trace in all panels is an average of 3–6 individual traces. *C*: summary plots show the average ACh and choline-evoked current amplitude in each cell type both before and after bath application of 20–50 nM MLA. Error bars represent standard errors. The numbers on the bars represent *n* values. All Scales: 50 pA, 100 ms except *A, bottom,* which is 100 pA, 100 ms.

of ACh. Of the remaining cells, two hilar interneurons and two molecular layer interneurons were not responsive (mean current amplitude collectively = 4.84 ± 1.66 pA), and two hilar interneurons produced small slow currents. One of these currents was not sensitive to antagonism by 50 nM MLA and the other was not tested. Extensive additional experiments would be necessary to determine if there are any common anatomical or histological features among these rare α7-negative hilar neurons, as no predictive features were apparent in our experiments.

Granule cells do not respond to focal somatic or dendritic application of ACh

We observed that like hilar interneurons, granule cells also failed to exhibit large spontaneous excitatory events when voltage clamped at –70 mV (Fig 4*B*, *top*). However, spontaneous inhibitory events that were mediated by GABA$_A$ receptors and blocked by bicuculline were readily apparent when voltage clamped at 0 mV (Fig. 4*B*, *bottom*). Although these cells were routinely identified by the presence of their soma in the granule cell layer, when current-clamp recordings were performed using a K-gluconate internal solution, granule cells could also often be distinguished from mossy cells based on their lack of a clear hyperpolarization-activated sag and from interneurons (hilar or molecular layer) by their pronounced fast afterhyperpolarization (Fig. 4*C*) (also see Lubke et al. 1998).

We found that granule cells are unresponsive to focal somatic application of ACh, regardless of whether their soma was located in the inner or outer granule cell layer. In 13 granule cells that received somatic applications of ACh while voltage clamped at –70 mV, the mean current amplitude was 4.8 ± 1.0 pA, a value comparable to that obtained from local circuit neurons in the presence of MLA (see examples in Fig. 4*D*). In 5 of the 13 granule cells tested, double-barreled application pipettes were used, and one barrel was loaded with 1 mM ACh, while the other barrel contained 1 mM glutamate. Each of those five cells responded to local application of glutamate (average current amplitude was 152 ± 49 pA, see example in Fig. 4*E*) and yet failed to respond to ACh delivered from the same location.

To examine the effect of focal application of ACh to granule cell dendrites, we filled granule cells with sulforhodamine 101 (Fig 4*F*). ACh was applied (1 mM, 1–20 ms) to visually identified dendrites from eight granule cells, and no single cell exhibited a reproducible response that exceeded the noise (average current amplitude was 5.6 ± 0.82 pA, see examples in Fig. 4*G*). In three cases, double-barreled application pipettes were used as before and dendritic responses to glutamate were readily observed (average current amplitude was 80 ± 39 pA, see example in Fig. 4*H*).

To further confirm that somatic and dendritic responses to focal application of ACh were indistinguishable from the
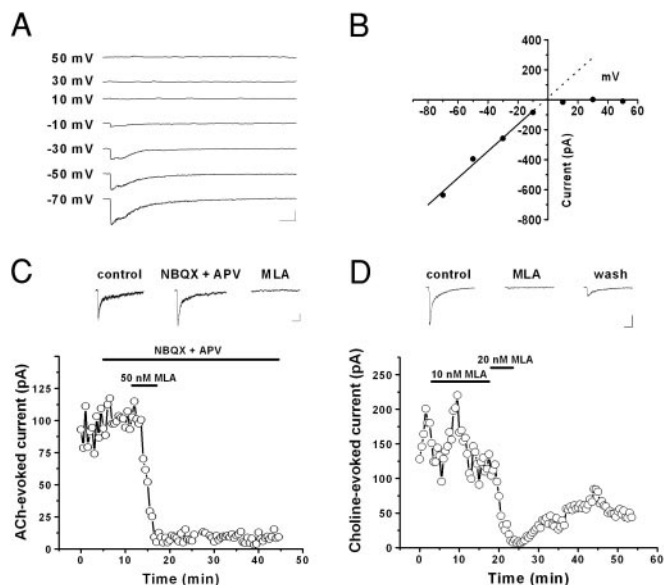
FIG. 3. Other features of ACh and choline-evoked responses. *A*: a sample current-voltage experiment performed on a hilar interneuron. Voltages were manually adjusted to the indicated values and 1 mM ACh was applied for 5 ms. Each trace is an average of 3–6 individual traces. *B*: peak data from the traces in *A* are plotted against voltage. A linear fit was performed to all data obtained at negative voltages (—), and extrapolated (- - -) to indicate a reversal potential near 0 mV. Strong inward rectification was observed at voltages positive of 0 mV. *C*: the time course of a typical experiment involving bath application of 10 μM NBQX, 40 μM APV, and 50 nM MLA. ○, the response to a single application of ACh, delivered at 30-s intervals. The time of NBQX, APV, and MLA applications is indicated (solid bar). *Top*: average of 3–6 individual traces taken from the indicated period. *D*: a comparable block (here of a choline-evoked response) could be obtained with lower MLA concentrations, although somewhat longer wash-in was required. Scale in *A*: 250 pA. 50 ms. Scale in *C*: 20 pA, 100 ms. Scale in *D*: 50 pA, 100 ms.

noise, we calculated the current integral of both types of responses over a 500-ms time period, starting with the time of ACh application and determined that neither were significantly different from a hypothesized mean value of 0 ($P = 0.60$, $n = 13$ for somatic responses, and $P = 0.11$, $n = 8$ for dendritic responses). This data are summarized in Fig. 4*I*. Overall, these results clearly indicated that granule cells lack robust expression of somatic or dendritic nAChRs.

Alpha7-mediated activation of subgranular hilar interneurons can produce IPSCs in granule cells

We next attempted to determine if cholinergic activation of nAChRs on local circuit neurons could lead to functional modulation of granule cell activity. Consistent with that hypothesis, we noted that long (0.5–1 s) puffs of ACh to the surface of the hilus or the molecular layer would occasionally produce long trains of IPSCs in granule cells voltage clamped at 0 mV in the presence of atropine, but in the absence of other antagonists (data not shown). There are a number of mono- and polysynaptic mechanisms that could potentially contribute to this effect. Therefore to better understand the response at a cellular level, we designed several experiments using brief focal applications of ACh.

We applied brief pulses of ACh to random subgranular interneurons (those within 50–60 μm of the granule cell layer, on the hilar side) in the hope of finding a synaptically connected pair. After numerous attempts, we found it quite diffi-

cult to drive IPSCs onto granule cells in this manner, although local application of glutamate from a double-barreled pipette was often effective. This suggested that local application of ACh was not producing an excitation of the subgranular interneurons that was sufficient to cause GABA release onto the granule cell. Therefore we recorded from nine additional subgranular interneurons using a K-gluconate internal solution and assessed the effects of local application of ACh in both voltage and current clamp directly. Consistent with previously published reports (Lubke et al. 1998), those nine interneurons had an average resting membrane potential of -61 ± 3.8 mV and an average input resistance of 205 ± 34.9 MΩ. When voltage clamped at -70 mV, they produced responses to local application of 1 mM ACh that were not significantly different from our earlier dataset, which had included interneurons from this subgranular zone as well as from deeper parts of the hilus (243 ± 58.7 vs. 191 ± 39.3 pA, respectively). In current-clamp mode, those same ACh applications produced an average depolarization of 17 ± 3.3 mV, and four of nine interneurons reached threshold for an action potential. Of those that did reach threshold, one to three action potentials were observed (data not shown). This result suggested that ACh applied to subgranular interneurons might drive IPSCs more effectively in the presence of slightly higher external KCl. Figure 5*B* show three consecutive traces during which glutamate was applied to a subgranular interneuron in our standard external solution. In each case, IPSCs were detected at the granule cell. In Fig. 5*B*, *middle*, it is apparent that ACh application failed to produce a similar response under those conditions. However, when the external KCl concentration was raised to 5.5 mM, local application of ACh produced IPSCs in the granule cell similar to those previously generated with glutamate. We therefore used an extracellular solution that contained 5 mM KCl for all remaining experiments (see METHODS). Using this external solution, connected pairs could be more readily identified using ACh application alone. Figure 5*C* (*left*) shows one such experiment in which local application of ACh to a subgranular interneuron produced clear IPSCs in a granule cell. In Fig. 5*C*, *right*, it is apparent that this effect of ACh was completely blocked by MLA and thus dependent on activation of α7-containing nAChRs. The results of four such experiments are summarized in Fig. 5*D*.

Overall, these results clearly demonstrate that cholinergic activation of α7-containing nAChRs on subgranular interneurons can lead to synaptic release of GABA onto granule cells. However, an additional hypothesis is that cholinergic activation of these receptors can also act cooperatively with other excitatory inputs to help modulate interneuron activity and thus granule cell function. We decided to test that hypothesis by determining whether activation of α7-containing nAChRs on subgranular interneurons would be more effective at enhancing electrically evoked IPSCs than at driving IPSCs directly.

Alpha7-mediated activation of subgranular interneurons enhances electrically evoked monosynaptic IPSCs recorded from granule cells

IPSCs were generated using a concentric bipolar stimulator placed in one of two positions in the molecular layer. For the first set of experiments, the stimulator was placed immediately across the granule cell layer from an identified
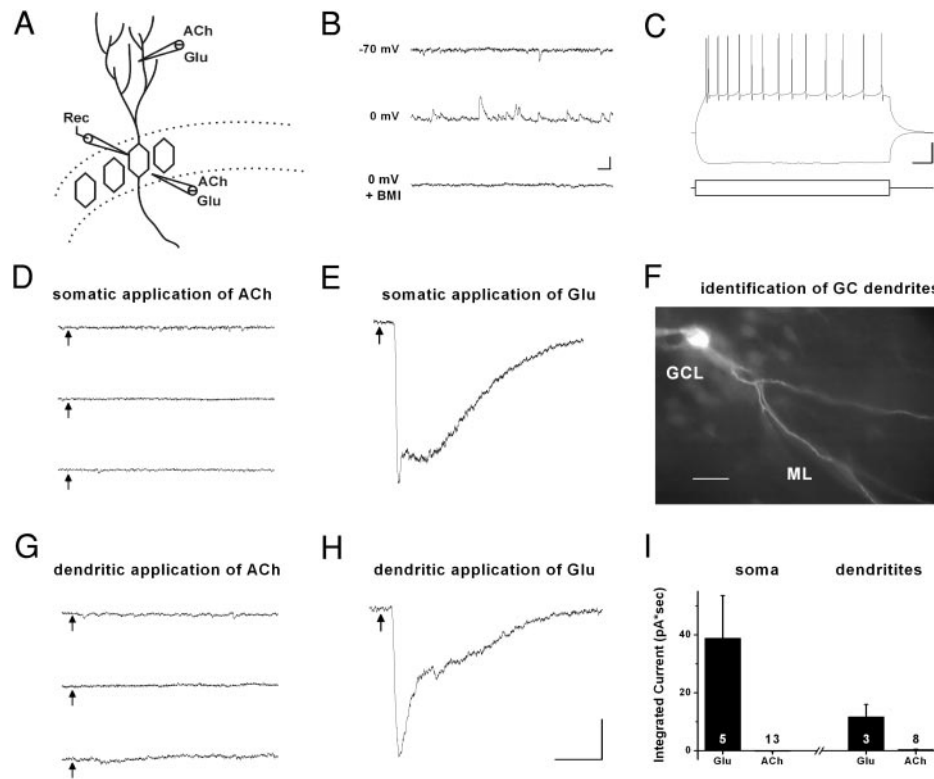
FIG. 4. Granule cells are unresponsive to focal somatic or dendritic application of ACh. *A*: schematic indicating how the experiments were performed. In this figure, and subsequent ones using variations of this diagram, the granule cell layer is indicated (- - -). Granule cells are represented by hexagons and the hilus is below the granule cell layer. The granule cell dendrites project into the molecular layer (above the granule cell layer). Granule cells were recorded using whole cell patch-clamp techniques with $CsMeSO_3$ internal and voltage clamped at –70 mV. Either 1 mM ACh or 1 mM glutamate was locally applied to either the cell body or dendrites of the granule cells using pressure ejection. *B*: characteristic features of granule cells. Granule cells lacked robust spontaneous excitatory events when voltage clamped at –70 mV (*top*), but showed clear outward currents at 0 mV (*middle*) that were blocked by the $GABA_A$ receptor antagonist bicuculline (30 μM, *bottom*). *C*: current-clamp recording using K-gluconate internal. Granule cells did not show a large hyperpolarization activated sag (*bottom,* −160 pA, 1 s) but did show a characteristic fast afterhyperpolarization after action potentials produced during a maintained depolarization (*top,* 160 pA, 1 s). *D*: sample data from 3 separate granule cells is shown to indicate that these neurons are not responsive to somatic application of ACh. Each trace indicates the average of 3–6 traces recorded from a separate granule cell. *E*: sample trace indicating that average response of a granule cell to somatic application of glutamate (1 mM). ↑, the times of glutamate application. *F*: granule cells are monopolar and have dendrites exclusively in the molecular layer as indicated in this photograph of a granule cell filled with sulforhodamine 101. This technique was used to identify granule cell dendrites for local application experiments. *G*: sample data from 3 separate granule cells indicates that these neurons do not produce clear responses to visually confirmed focal dendritic application of ACh. Each trace indicates the average of 3–6 traces recorded from a separate granule cell. ↑, time of ACh application. *H*: the average response of a single granule cell to visually confirmed dendritic application of glutamate via a double-barreled application pipette. ↑, the time of glutamate application. *I*: a summary plot shows the average response to glutamate vs. the average response to ACh for both somatic and dendritic experiments. The response is expressed as the current integral calculated over a 500-ms time period, starting with time of ACh application. In each case, the response to ACh was not significantly different from the background noise. The numbers on (or above) the bars indicate the n values. Scale in *B*: 25 pA, 100 ms. Scale in *C*: 20 mV, 100 ms. Scale in *H* represents: 40 pA, 100 ms in *D,G,* and *H,* and 80 pA, 200 ms in *E*. Scale in *F*: 20 μm.

subgranular interneuron. This placement was chosen to maximize the probability of generating a monosynaptic IPSC by direct activation of the interneuron dendrites (Fig. 6*A*). Indeed, when low-intensity stimulation was delivered from this location, monosynaptic IPSCs could often be recorded from a nearby granule cell voltage clamped at 0 mV. The monosynaptic nature of these responses was indicated by the short latency between the stimulus and the onset of the response (1.2 ± 0.22 ms, $n = 7$) and also by insensitivity to blockade by glutamate receptor antagonists (Fig. 6*B*). Electrical stimuli were delivered at 15 or 20-s intervals, and ACh was co-applied in the subgranular zone near an interneuron soma with every other stimulus (see diagram in Fig. 6*A*). Under those conditions, we were able to observe a clear ACh-mediated enhancement of the monosynaptic IPSC (Fig. 6*C*). Bath application of 50 nM MLA revealed that this effect of ACh was entirely dependent on activation of α7-containing nAChRs (Fig. 6*D*). We also demonstrated that the NBQX- and APV-insensitive response that had been enhanced by ACh application was indeed a GABAergic IPSC by blocking it with bath application of 30 μM bicuculline (Fig. 6*E*). A similar series of experiments was successfully conducted in eight separate granule cells. Overall, co-application of ACh increased the amplitude of the monosynaptic IPSC to an average of 121 ± 5.99% of control. In the presence of MLA, this effect was completely eliminated. Co-application of ACh produced IPSCs with peak amplitudes of 101 ± 4.61% of control (see summary, Fig. 8*A*).
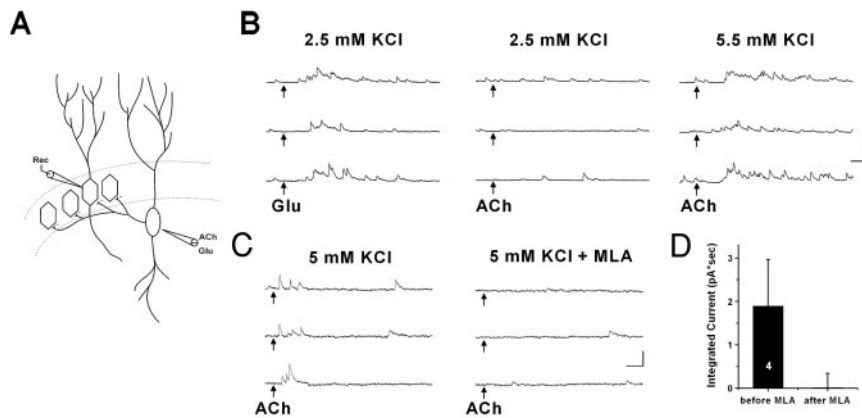
FIG. 5. Alpha7 mediated activation of hilar interneurons produces inhibitory postsynaptic currents (IPSCs) in granule cells. *A*: schematic indicating the experimental design. All symbols are identical to those described for Fig. *4A*, and a hilar neuron has been added. Granule cells were voltage clamped at 0 mV while either ACh (1 mM) or glutamate (1 mM) was applied to the soma of a nearby subgranular interneuron (oval). *B, left*: glutamate applied to the hilar interneuron produces IPSCs in the granule cell. ACh application failed to reproduce this effect (*middle*) until external KCl was raised to 5.5 mM (*right*). *C*: in 5 mM KCl, we occasionally found connected pairs using a single-barrel ACh application pipette. *Left*: ACh application to a subgranular interneuron produced IPSCs in the granule cell. *Right*: this effect was completely blocked by bath application of 50 nM MLA. *D*: summary plot of data from four similar experiments. The current integral was calculated over a 500-ms time period, starting with the time of ACh application. MLA completely blocked ACh-induced IPSCs. In *B* and *C*, each set of 3 traces shows individual sweeps recorded consecutively at 30-s intervals. Arrows indicate time of ACh application or glutamate application. Scale in *B*: 100 pA, 100 ms. Scale in *C*: 25 pA, 50 ms.

Alpha7-mediated activation of subgranular interneurons enhances electrically evoked disynaptic IPSCs recorded from granule cells

Another question of interest is whether ACh application to a subgranular interneuron can functionally enhance the effect of synaptically released glutamate. To address that question, it was necessary to generate disynaptic IPSCs. This was accomplished by moving the stimulator 50–200 μm away from a target interneuron, parallel to the granule cell layer (Fig. 7*A*).

This allowed us to activate glutamatergic inputs to subgranular interneurons that arrive from the entorhinal cortex and run through the molecular layer. However, one consequence of this arrangement was that in addition to driving glutamatergic activation of subgranular interneurons, we often also activated additional excitatory inputs to the granule cell. The effect of this monosynaptic excitatory pathway was largely eliminated by voltage clamping the granule cell at 0 mV. Figure 7*B* shows the response of a granule cell voltage clamped at –70 mV to
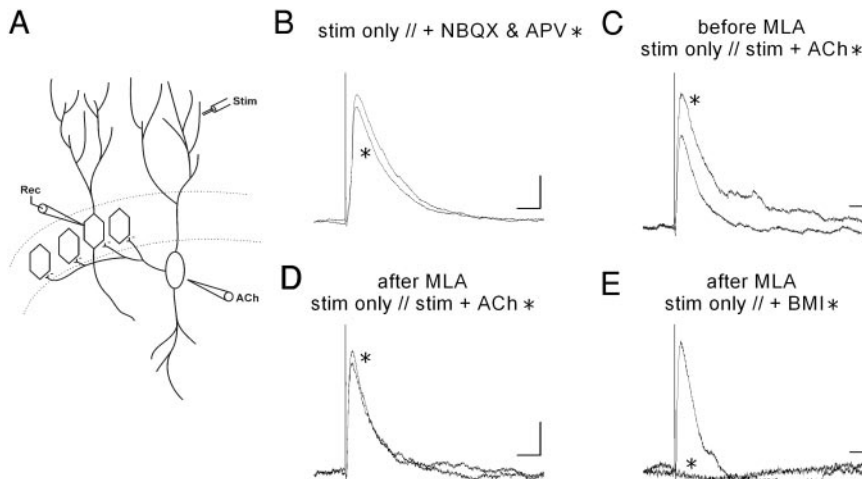

FIG. 6. Alpha7-mediated activation of subgranular interneurons enhances monosynaptic IPSCs recorded from granule cells. *A*: schematic indicating the experimental design. Symbols are as previously described (Figs. 3*A* and 4*A*). Recordings were made from granule cells voltage clamped at 0 mV. Subgranular interneurons were activated by electrical stimulation from a bipolar stimulator placed directly across the granule cell layer from the soma, with and without concurrent application of ACh (1 mM) to the soma. *B*: stimulation (.1 ms, 50–300 μA) produced IPSCs that were not sensitive to 10 μM NBQX and 40 μM APV. *C*: co-application of ACh (10 ms) to the soma enhanced the amplitude of the monosynaptic IPSC. *D*: this effect of ACh was eliminated by bath application of 50 nM MLA. *E*: the monosynaptic IPSC that remained in the presence of NBQX, APV, 5 μM atropine, and MLA was totally blocked by 30 μM BMI, indicating that it was mediated by GABA$_A$ receptors. Traces shown in *B–E* are all averages of 10 individual sweeps and were recorded from the same neuron. In *C* and *D*, stimulation was delivered every 15 s, and co-application of ACh occurred with every other stimulus. Sweeps marked with * correspond to conditions marked with * in the labels. Scale in *A*: 50 pA, 50 ms. Scale in *C–E*: 10 pA, 50 ms.
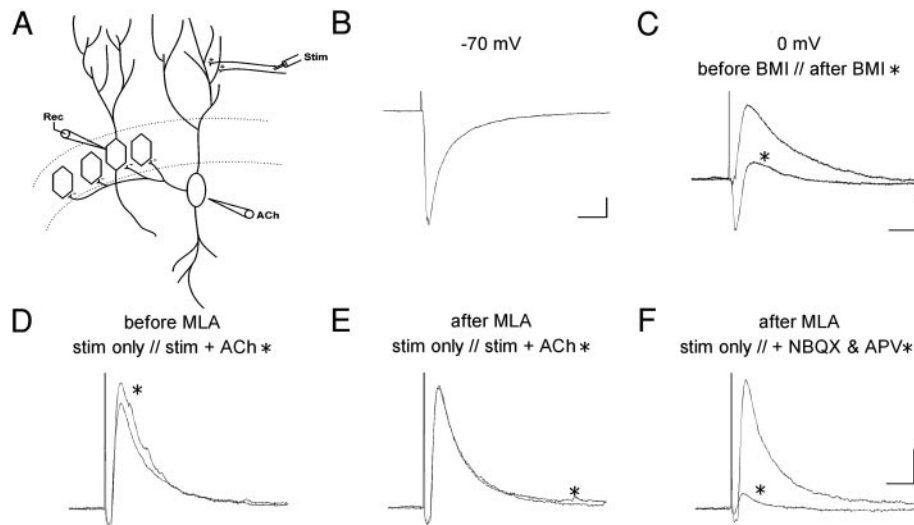
FIG. 7. Alpha7-mediated activation of subgranular interneurons enhances disynaptic IPSCs recorded from granule cells. *A*: schematic indicating the experimental design. These experiments were conducted as those in Fig. 6 except the stimulator was not placed directly across the granule cell layer from a target interneuron, but rather 60–200 μm away, to activate glutamatergic afferents in the perforant path. *B*: an EPSC is created in a granule cell voltage clamped at –70 mV by stimulation of the perforant path. *C*: the same cell as in *B* before and after treatment with 30 μM BMI, but voltage clamped at 0 mV. A clear GABA$_A$-mediated IPSC is present at 0 mV despite activation of monosynaptic excitatory inputs to the GC. Note the longer latency of this response as opposed to the EPSC in *A* (5.1 vs. 1.5 ms, respectively). This is one indication that the IPSC is likely disynaptic. *D*: ACh (1 mM) enhances the effect of a presumably disynaptic IPSC. *E*: the effect of ACh is eliminated by bath application of 50 nM MLA. *F*: the disynaptic nature of the IPSC is confirmed by blocking it with bath application of 10 μM NBQX and 40 μM APV. Traces shown in *B–F* are all averages of 10 individual sweeps. Those in *B* and *C* were recorded from the same granule cell, while those in *D–F* were from another cell. In *D* and *E* stimulation was delivered every 15 s, and co-application of ACh (15 ms) occurred with every other stimulus. Sweeps marked with * correspond to conditions marked with * in the labels. Scale in *B* and *C*: 25 pA, 25 ms. Scale in *F*: 20 pA, 25 ms also applies to *D* and *E*.

stimulation of the perforant path. Figure 7*C* shows the response of the same granule cell to the same stimulus when voltage clamped at 0 mV. Note that a clear outward current was apparent at 0 mV, that this current had a longer latency than the monosynaptic current in Fig. 7*B* (5.1 vs. 1.5 ms, respectively) and that it was almost entirely blocked by BMI, indicating that it was mediated by GABA$_A$ receptors. The remaining current was the same glutamatergic current seen in Fig. 7*A* but now greatly reduced (note the different scale) because the cell was voltage clamped near the reversal potential of nonselective cation channels. This data demonstrate that stimulation of the perforant path will produce a relatively pure GABA$_A$ mediated IPSC in a granule cell voltage clamped at 0 mV despite activation of monosynaptic excitatory inputs to the granule cell. Ultimately the disynaptic nature of these BMI-sensitive IPSCs was indicated by their susceptibility to blockade by glutamate receptor antagonists (see following text), but they could also be identified with a high degree of accuracy by the latency between the stimulus artifact and the rising phase of the response (4.5 ± 0.99 ms, n = 5).

Our results indicate that this type of disynaptic IPSC can also be enhanced by application of ACh near the soma of a subgranular interneuron (Fig. 7*D*). For this experiment, the perforant path was stimulated at 15-s intervals, and ACh was co-applied on every other stimulus as in previous experiments. The clear effect of ACh was also dependent on activation of α7-containing nAChRs as indicated by the complete block produced by bath application of MLA (Fig. 7*E*). Finally, we show that the IPSC that was enhanced by ACh in Fig. 7*D* was disynaptic by blocking it with glutamate receptor antagonists (Fig. 7*F*). A similar series of experiments was successfully

conducted in five separate granule cells. Overall, co-application of ACh increased the amplitude of the disynaptic IPSC to 136 ± 17.9% of control. In those same five cells, co-application of ACh had no effect on the disynaptic IPSC amplitude in the presence of MLA (measured as 99 ± 4.3% of control). These data are summarized in Fig. 8*B*. In addition to the 13 experiments summarized in Fig. 8 in which the IPSC was explicitly identified as mono- or disynaptic and challenged with MLA, we observed this basic effect of ACh in two other cases that were not explicitly tested with NBQX and APV. The latency of those responses suggested that one was monosynaptic and the other was disynaptic.

DISCUSSION

This study demonstrates that functional nAChRs containing the α7 subunit are expressed by morphologically and physiologically identified molecular layer interneurons, hilar interneurons, and mossy cells in the dentate gyrus. We also show that the principal neurons of the dentate, the granule cells, do not produce clear responses to somatic application of ACh or to focal application on their dendrites. All of these results confirm and extend the same basic dichotomy previously reported in both the dentate gyrus (Jones and Yakel 1997) and in CA1 (Frazier et al. 1998b; Jones and Yakel 1997; McQuiston and Madison 1999), whereby there is robust expression of α7-containing nAChRs on local circuit neurons but not on principal neurons. Thus these results further strengthen the hypothesis that cholinergic afferentation of nAChRs in the hippocampus and the dentate gyrus is likely to contribute to the regulation of principal cell output primarily through modula-
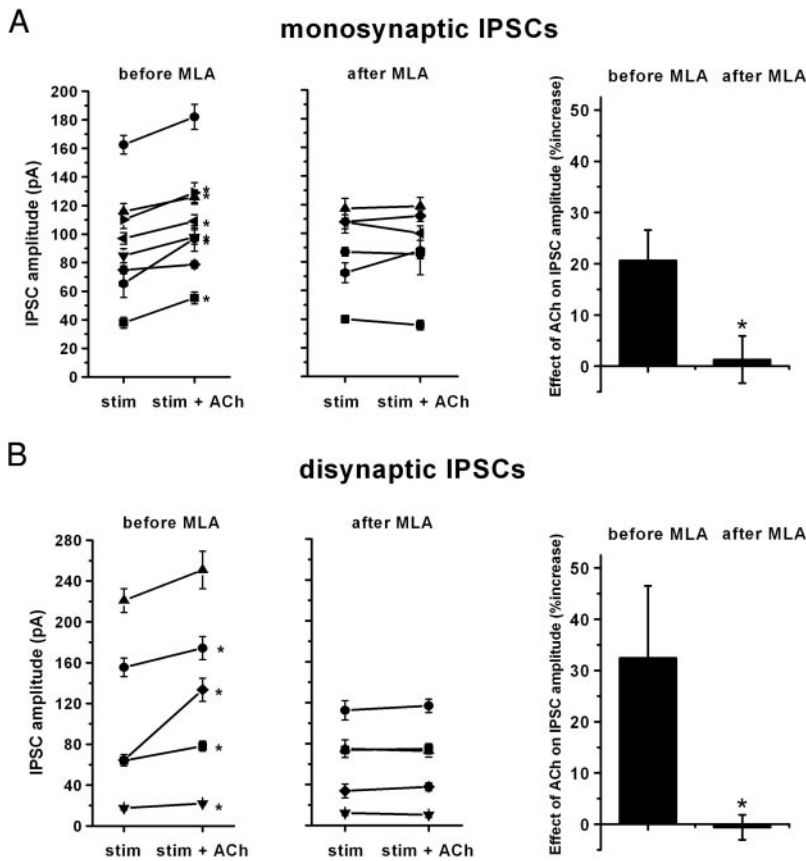
FIG. 8. Summary of ACh-mediated enhancement of mono- and disynaptic IPSCs. *A*: the ACh-mediated enhancement of monosynaptic IPSCs on a cell-by-cell basis. Data are only plotted from those experiments where IPSCs were explicitly identified as monosynaptic by demonstrating minimal sensitivity to blockade by 10 μM NBQX and 40 μM APV. *Left*: each pair of data points represents data from a separate granule cell. The average amplitude of the monosynaptic IPSC (and standard error) is shown both with and without co-application of ACh. Each data point represents 10–20 sweeps from an experiment where stimuli were delivered to the molecular layer, with ACh co-application occurring on every other sweep. *Middle*: the same experiment repeated on the same cells after bath application of 50 nM MLA. The symbols used to identify each cell correspond to those used on *left*. *Right*: summary plot of this data indicating that on average ACh application in the subgranular region increased the monosynaptic IPSC by 21 $\pm$ 6.0%. This effect was eliminated in the presence of MLA. *B*: the ACh-mediated enhancement of disynaptic IPSCs on a cell-by-cell basis. Data are only plotted from those experiments where IPSCs were explicitly identified as disynaptic by demonstrating sensitivity to blockade by 10 μM NBQX and 40 μM APV. In all other respects, data are presented exactly as in *A,* although 1 experiment (▼) involved ACh application to a molecular layer rather than a subgranular interneuron. *, a statistically significant difference in the average IPSC amplitude ($P \leq 0.05$ on a 1-tailed, paired *t*-test).

tion of local circuit function. Recently, the results of Ji et al. (2001) have suggested a potential exception to this generalization, i.e., that previously overlooked and sparsely expressed α7-containing nAChRs on CA1 pyramidal cell dendrites play an important role in the induction of long-term potentiation. Our results indicate that brief focal application of ACh to visually identified granule cell dendrites does not produce a response that can be reliably detected in the soma. It is possible that more widespread application of cholinergic agonists to granule cell dendrites would help to expose sparse expression of nAChRs similar to that reported in CA1 pyramidal cells by Ji et al. (2001) and that activation of such receptors could be functionally significant. However, our results also indicate that in doing such experiments it will be essential to carefully control for potential mono- and polysynaptic mechanisms that are initiated by broad application of cholinergic agonists.

Because we found that high levels of functional nAChRs in the dentate gyrus are expressed by local circuit neurons, we also tested the hypothesis that cholinergic activation of subgranular interneurons can contribute to the regulation of granule cell excitability. Specifically, we demonstrated that focal application of ACh to these neurons can drive IPSCs onto granule cells, that it can enhance an electrically evoked monosynaptic IPSC, and, perhaps most importantly, that it can enhance the ability of synaptically released glutamate to produce granule cell inhibition. Because the ACh-evoked responses that we recorded directly from mossy cells, hilar interneurons, and molecular layer interneurons were unaffected by glutamate receptor antagonists and/or TTX, we conclude that those responses were mediated by somatic nAChRs and not by nAChRs acting as presynaptic heteroreceptors to facil-

itate the release of other excitatory transmitters. This finding is consistent with previous reports concerning expression of α7 nAChRs by local circuit neurons in CA1 (Frazier et al. 1998b; McQuiston and Madison 1999). However, similar controls were not possible during experiments that involved recording mono- and disynaptic IPSCs directly from granule cells, and thus the question may arise as to whether activation of presynaptic α7-containing nAChRs on GABAergic terminals contributed to the ACh-mediated enhancement in mono- and disynaptic IPSCs reported here. Several lines of evidence argue against that possibility. In considering the question, it is important to note that all of the experiments summarized in Fig. 8 involved stimulation in the molecular layer. Under those conditions, we were able to observe an ACh-mediated enhancement of the mono- or disynaptic IPSC in approximately one of every five granule cells tested. That ratio is indicative of the difficulty involved in activating the same subpopulation of interneurons with two nonsaturating stimuli. Interestingly, when the stimulator was placed in the hilus, monosynaptic IPSCs were routinely generated, but we were able to observe an ACh-mediated enhancement of the IPSC in only 1 of >20 attempts (data not shown). One probable explanation for that observation is that a stimulator placed in the hilus is far more likely to activate GABAergic axons of septal afferents than a stimulator placed in the molecular layer, which will be more likely to activate the dendrites of hilar interneurons or the glutamatergic afferents of the perforant path. If facilitation of GABA release by presynaptic α7-containing nAChRs played a prominent role in our experiments, we would expect that the ACh-mediated enhancement of the monosynaptic IPSC would be as easy or easier to detect with hilar stimulation as with

molecular layer stimulation. As that was not the case, we conclude that ACh-mediated facilitation of GABA release from presynaptic terminals is unlikely to have been a major factor in our experiments. The fact that the drug application pipette was generally between 30 and 100 μm away from the granule cell soma and on the opposite side of the granule cell layer from the dendrites further strengthens this conclusion. This interpretation is also consistent with previous reports that ACh-mediated facilitation of GABA release in area CA1 of the hippocampus is TTX-sensitive (Albuquerque et al. 1998). Nevertheless, it seems quite possible that future studies using different experimental approaches may uncover clear functional roles for presynaptic nAChRs in the dentate gyrus (Gray et al. 1996; but see Vogt and Regehr 2001).

Overall, our results suggest the possibility of a complex interplay between glutamatergic inputs from the entorhinal cortex and cholinergic inputs from the medial septum in the normal regulation of granule cell function. It is tempting to speculate that endogenous activation of α7-containing nAChRs by synaptically released ACh might similarly provide direct and/or cooperative modulation of inhibitory circuits within the dentate gyrus in vivo. This hypothesis is fueled not only by the results presented in this report but also by the fact that similar receptors on interneurons in area CA1 have been shown to be activated by synaptic release of endogenous ACh (Alkondon et al. 1998; Frazier et al. 1998a) and by the recent observation that septohippocampal cholinergic afferents form conventional synapses on hilar neurons (Deller et al. 1999; Dougherty and Milner 1999). However, it is important to note that we also show in this manuscript that the α7-containing nAChRs expressed by hilar neurons can be activated by somatic application of choline (10 mM) and desensitized by physiologically relevant concentrations of bath-applied choline (40 μM). These observations are consistent with previous reports regarding the effects of choline on α7-containing nAChRs expressed in other systems (Alkondon et al. 1997; Frazier et al. 1998b; Papke et al. 1996; Uteshev et al. 2002) and suggest the possibility that choline may modulate nAChR function through volume transmission in vivo. Thus it will be extremely important for future studies to examine the extent to which fast synaptic and volume transmission contribute to the normal activation and/or desensitization of α7-containing nAChRs in the dentate gyrus. A better understanding of each of these functional modalities will be essential in developing more effective therapeutic strategies for coping with age-related degeneration of the septohippocampal cholinergic system.

While the downstream consequences of cholinergic activation of mossy cells remain, for the moment, untested, several interesting possibilities exist. The local application studies presented here provide the first demonstration of robust somatic expression of functional nAChRs by any glutamatergic cell type in the hippocampus or dentate gyrus. In addition to being glutamatergic (Soriano and Frotscher 1994), mossy cells are also unusual among local circuit neurons in the dentate in that their axons project along the septotemporal axis of the hippocampus and form a large portion of the commissural/associational projection to the inner molecular layer (Scharfman et al. 1990). This significantly complicates the study of synaptic circuits involving mossy cells as complete circuits may not exist within the hippocampal slice (Scharfman et al.

1990). However, ultrastructural studies have demonstrated that the axons of mossy cells likely form dense synaptic contacts with granule cell dendrites in the inner molecular layer (Buckmaster et al. 1996) and may also have synapses on inhibitory interneurons (Scharfman et al. 1990). These features of mossy cells, coupled with the recent observation that they are directly innervated by septohippocampal cholinergic afferents (Deller et al. 1999), and our demonstration that they express functional nAChRs, lead us to hypothesize that cholinergic input to mossy cells could be an important factor contributing to a role in the regulation and possibly synchronization of granule cell activity. Considered in combination with our results concerning cholinergic modulation of inhibitory circuits in the dentate, we believe that the septohippocampal cholinergic projection and the functional nAChRs described here could ultimately have a prominent role not only in the generation of hippocampal theta rhythms and memory formation but also in other areas that depend on tight control over granule cell activity, such as the modulation of seizure susceptibility and the etiology of temporal lobe epilepsy.

REFERENCES

Albuquerque EX, Pereira EF, Braga MF, and Alkondon M. Contribution of nicotinic receptors to the function of synapses in the central nervous system: the action of choline as a selective agonist of alpha 7 receptors. *J Physiol* 92: 309–316, 1998.

Alkondon M, Pereira EFR, and Albuquerque EX. alpha-Bungarotoxin- and methyllycaconitine-sensitive nicotinic receptors mediate fast synaptic transmission in interneurons of rat hippocampal slices. *Brain Res* 810: 257–263, 1998.

Alkondon M, Pereira EFR, Cortes WS, Maelicke A, and Albuquerque EX. Choline is a selective agonist of α7 nicotinic acetylcholine receptors in the rat brain neurons. *Eur J Neurosci* 9: 2734–2742, 1997.

Aramakis VB and Metherate R. Nicotine selectively enhances NMDA receptor-mediated synaptic transmission during postnatal development in sensory neocortex. *J Neurosci* 18: 8485–8495, 1998.

Bertrand D. Neuronal nicotinic acetylcholine receptors: their properties and alterations in autosomal dominant nocturnal frontal lobe epilepsy. *Rev Neurol* 155: 457–462, 1999.

Buckmaster PS, Strowbridge BW, Kunkel DD, Schmiege DL, and Schwartzkroin PA. Mossy cell axonal projections to the dentate gyrus molecular layer in the rat hippocampal slice. *Hippocampus* 2: 349–362, 1992.

Buckmaster PS, Wenzel HJ, Kunkel DD, and Schwartzkroin PA. Axon arbors and synaptic connections of hippocampal mossy cells in the rat *in vivo. J Comp Neurol* 366: 271–292, 1996.

Buhler AV and Dunwiddie TV. alpha7 nicotinic acetylcholine receptors on GABAergic interneurons evoke dendritic and somatic inhibition of hippocampal neurons. *J Neurophysiol* 87: 548–557, 2002.

Deller T, Katona I, Cozzari C, Frotscher M, and Freund TF. Cholinergic innervation of mossy cells in the rat fascia dentata. *Hippocampus* 9: 314–320, 1999.

Descarries L, Gisiger V, and Steriade M. Diffuse transmission by acetylcholine in the CNS. *Prog Neurobiol* 53: 603–625, 1997.

Dougherty KD and Milner TA. Cholinergic septal afferent terminals preferentially contact neuropeptide Y-containing interneurons compared to parvalbumin-containing interneurons in the rat dentate gyrus. *J Neurosci* 19: 10140–10152, 1999.

Elmslie FV, Rees M, Williamson MP, Kerr M, Kjeldsen MJ, Pang KA, Sundqvist A, Friis ML, Chadwick D, Richens A, Covanis A, Santos M, Arzimanoglou A, Panayiotopoulos CP, Curtis D, Whitehouse WP, and

Gardiner RM. Genetic mapping of a major susceptibility locus for juvenile myoclonic epilepsy on chromosome 15q. *Hum Mol Genet* 6: 1329–1334, 1997.

Fabian-Fine R, Skehel P, Errington ML, Davies HA, Sher E, Stewart MG, and Fine A. Ultrastructural distribution of the alpha7 nicotinic acetylcholine receptor subunit in rat hippocampus. *J Neurosci* 21: 7993–8003, 2001.

Frazier CJ, Buhler AV, Weiner JL, and Dunwiddie TV. Synaptic potentials mediated via alpha-bungarotoxin-sensitive nicotinic acetylcholine receptors in rat hippocampal interneurons. *J Neurosci* 18: 8228–8235, 1998a.

Frazier CJ, Rollins YD, Breese CR, Leonard S, Freedman R, and Dunwiddie TV. Acetylcholine activates an α-bungarotoxin-sensitive nicotinic current in rat hippocampal interneurons, but not pyramidal cells. *J Neurosci* 18: 1187–1195, 1998b.

Gray R, Rajan AS, Radcliffe KA, Yakehiro M, and Dani JA. Hippocampal synaptic transmission enhanced by low concentrations of nicotine. *Nature* 383: 713–716, 1996.

Hatton GI and Yang QZ. Synaptic potentials mediated by alpha 7 nicotinic acetylcholine receptors in supraoptic nucleus. *J Neurosci* 22: 29–37, 2002.

Jackson MB and Scharfman HE. Positive feedback from hilar mossy cells to granule cells in the dentate gyrus revealed by voltage-sensitive dye and microelectrode recording. *J Neurophysiol* 76: 601–616, 1996.

Ji D and Dani JA. Inhibition and disinhibition of pyramidal neurons by activation of nicotinic receptors on hippocampal interneurons. *J Neurophysiol* 83: 2682–2690, 2000.

Ji D, Lape R, and Dani JA. Timing and location of nicotinic activity enhances or depresses hippocampal synaptic plasticity. *Neuron* 31: 131–141, 2001.

Johnston D and Amaral DG. Hippocampus. In: *The Synaptic Organization of the Brain,* Shepherd GM. New York: Oxford Univ. Press, 1998, p. 417–458.

Jones S and Yakel JL. Functional nicotinic ACh receptors on interneurones in the rat hippocampus. *J Physiol* 504: 603–610, 1997.

Levy RB and Aoki C. Alpha7 nicotinic acetylcholine receptors occur at postsynaptic densities of AMPA receptor-positive and -negative excitatory synapses in rat sensory cortex. *J Neurosci* 22: 5001–5015, 2002.

Lubke J, Frotscher M, and Spruston N. Specialized electrophysiological properties of anatomically identified neurons in the hilar region of the rat fascia dentata. *J Neurophysiol* 79: 1518–1534, 1998.

McQuiston AR and Madison DV. Nicotinic receptor activation excites distinct subtypes of interneurons in the rat hippocampus. *J Neurosci* 19: 2887–2896, 1999.

Papke RL, Bencherif M, and Lippiello P. An evaluation of neuronal nicotinic acetylcholine receptor activation by quaternary nitrogen compounds indicates that choline is selective for the α7 subtype. *Neurosci Lett* 213: 201–204, 1996.

Radcliffe KA, Fisher JL, Gray R, and Dani JA. Nicotinic modulation of glutamate and GABA synaptic transmission in hippocampal neurons. *Ann NY Acad Sci* 868: 591–610, 1999.

Scharfman HE. Differentiation of rat dentate neurons by morphology and electrophysiology in hippocampal slices: granule cells, spiny hilar cells and aspiny "fast-spiking" cells. *Epilepsy Res Suppl* 7: 93–109, 1992.

Scharfman HE, Kunkel DD, and Schwartzkroin PA. Synaptic connections of dentate granule cells and hilar neurons: results of paired intracellular recordings and intracellular horseradish peroxidase injections. *Neuroscience* 37: 693–707, 1990.

Scharfman HE and Schwartzkroin PA. Electrophysiology of morphologically identified mossy cells of the dentate hilus recorded in guinea pig hippocampal slices. *J Neurosci* 8: 3812–3821, 1988.

Soriano E and Frotscher M. Mossy cells of the rat fascia dentata are glutamate-immunoreactive. *Hippocampus* 4: 65–69, 1994.

Uteshev VV, Meyer EM, and Papke RL. Regulation of neuronal function by choline and 4OH-GTS-21 through {alpha}7 nicotinic receptors. *J Neurophysiol* 89: 1797–1806, 2003.

Vogt KE and Regehr WG. Cholinergic modulation of excitatory synaptic transmission in the CA3 area of the hippocampus. *J Neurosci* 21: 75–83, 2001.